

Stochastic analysis of time-series related to ocean acidification

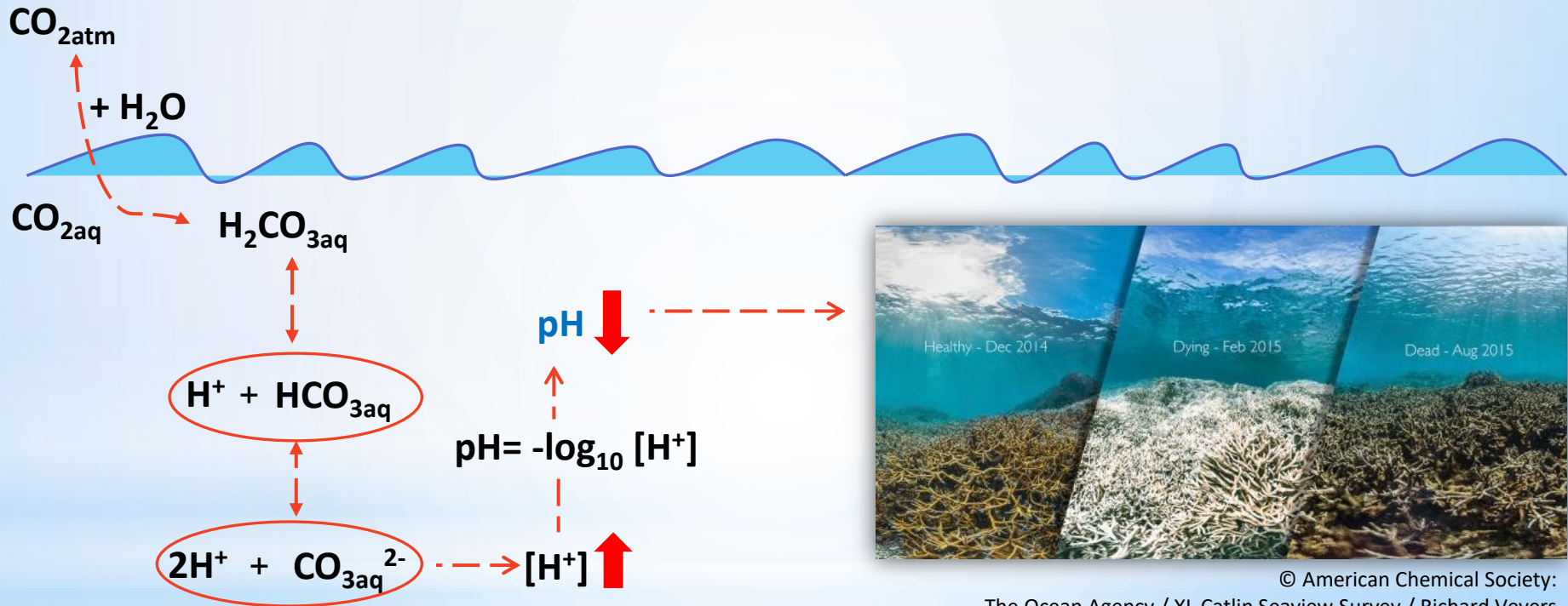
G. Vagenas, T. Iliopoulou, P. Dimitriadis, D. Koutsoyiannis

Affiliation: National Technical University of Athens, School of Civil Engineering,
Department of Water Resources and Environmental Engineering, Athens, Greece

European Geosciences Union
General Assembly
(April -2021)

“Ocean acidification (OA): The other CO₂ problem” ^[1]

The phenomenon: OA is described as the constant increase of atmospheric carbon dioxide (CO_{2atm}) which reduces ocean pH and causes wholesale shifts in seawater carbonate chemistry^[1].



Objective: We perform time-series analysis focused on temporal changes in month and annual time lag, in order to detect the interaction between each variable element along with the seasonality effect.

Methodology (1)

Data (Time-series) specifications:

Variables

- 1) Aquatic measurements: Hawaii Ocean Time series (HOT) [2]

CO_{2aq}: The mean surface seawater CO₂ partial pressure, in μatm , calculated from DIC* and TA** at in situ temperature.

PH: The mean surface seawater pH, calculated from DIC and TA at in situ temperature, on the total scale.

Temperature: The mean surface in situ seawater temperature, in $^{\circ}\text{C}$.

- 2) Atmospheric measurements: (Mauna Loa, Hawaii) [3]

CO_{2atm}: Surface CO₂ in-situ measurements (ppm)

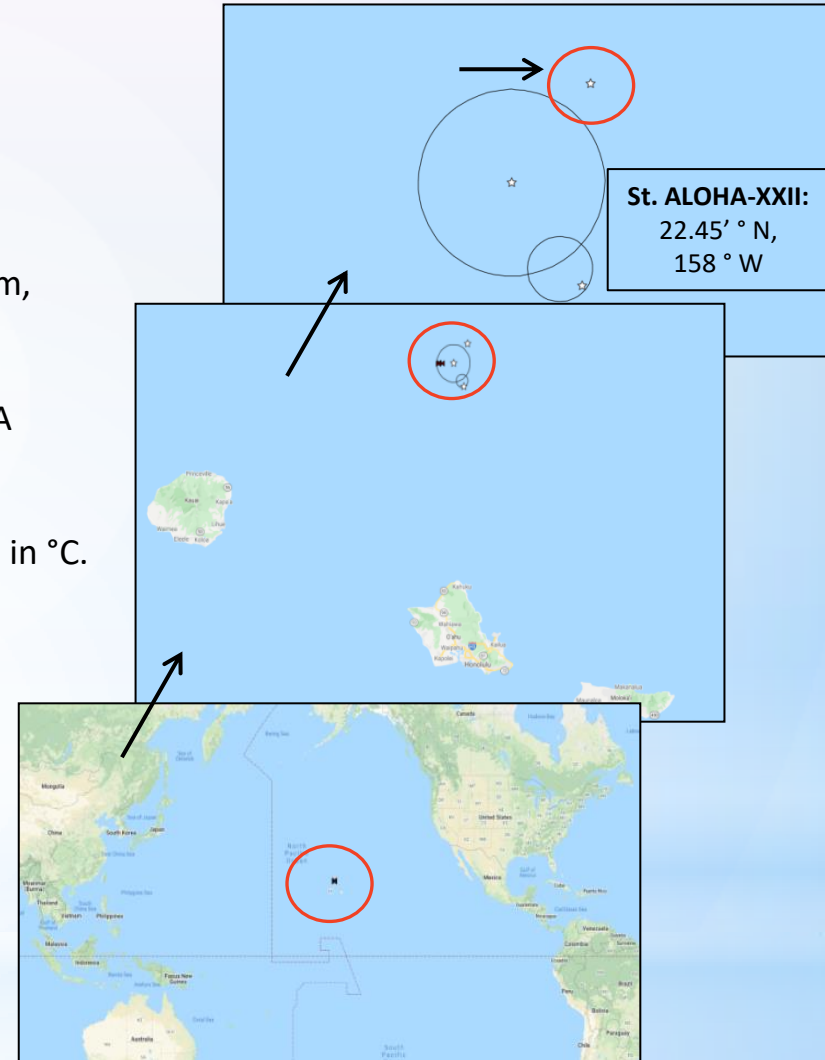
Location: North Pacific Ocean (Hawaiian Archipelago)

Year Range

October 1988 – October 2018 (30 years)

Time-step (Δt)

Monthly measurements



*Dissolved Inorganic Carbon

**Total Alkalinity

Methodology (2)

Time series procedures-functions (Analysis steps):

1) Linear Interpolation

Step standardization at y (NA value), at a given x, was operated with the use of the following formula^[4]:

$$y(x) = y_i + (y_{i+1} - y_i) \frac{x - x_i}{x_{i+1} - x_i}, \quad x_i < x < x_{i+1}$$

2) Cross-correlation function (CCF)

CCF (r_{xy}) at a discrete time k was calculated according to the formula of^[5,6]:

$$r_{x,y}^k = \frac{\sum_{s=\max(1,-t)}^{\min(n-t,n)} (x_i(s+t) - \bar{x}_i)(x_j(s) - \bar{x}_j)}{\sqrt{SD_x SD_y}}$$

X_i =predictor variable (x) $c_{i,j}$ =CCF function
 X_j =response variable (y) n =sample size
 \bar{x}_j =expected value of x t =time lag
 \bar{x}_i =expected value of y SD =st. deviation

The statistical significance of the CCF was approximately approached with the 95% confidence intervals ($CI_{95\%}$) of the CCF, estimated as follows^[6]:

$$CI_{95\%} = -\frac{1}{n} \pm \frac{2}{\sqrt{n}}$$

where n is the number of data points used in the calculation of the CCF, and the $CI_{95\%}$ equations which are depicted as dashed blue lines in the CCF plots. We utilized the simplified tool of CCF since it represent one of the most informative indicators in terms of directionality^[7]. In cases where significant time dependence was observed, Monte-Carlo simulation (MCS) was applied to determine the 95% confidence intervals through the fundamental stochastic Markovian process AR(1) depicted as purple dot-dashed lines.

Methodology (2)

Time series procedures (Analysis steps):

3) Moving Average (Rolling Monthly Average)

A simple (unweighed) moving average (MA) was calculated successively for complete annual time series (Jan-Dec) for monthly (q=2 month) and annual (q=12 month) time step:

$$MA_q(i) = \frac{X_{n-k+1} + X_{n-k+2} + \dots + X_n}{q} = \frac{1}{q} \sum_{i=n-q+1}^n x_i$$

q=rolling grade (months)
n=sample size
 X_i =x value
k=dynamic variable (initial k=0)
 \underline{x} =random variable

4) Annual differencing - Δ (Rolling Annual Difference)

Annual differencing $\Delta(\tilde{x})$ was calculated successively for complete annual time series as follows in order to eliminate periodicity^[7]:

$$\tilde{x}_{k,v} := x_{k+v} - x_v$$

v=time step differencing

5) Seasonality effect (SE) at various time lags (q)^[7]

$$SE_q(i) = X_t(i) - MA_q(i)$$

X_t =Time series

Methodology (2)

Time series procedures (Analysis steps):

6) Empirical climacogram (Monthly & Annual) & Hurst parameter

Climacogram (GR: κλίμαξ~climax; EN: scale) is defined as the variance of the averaged process at discrete time scale κ: [8]

$$\rho_{\kappa} := \text{var} \left[\frac{X_{\kappa}}{\kappa\sigma} \right] = \frac{\gamma_{\kappa}}{\gamma_1}, \quad \gamma_{\kappa} := \text{var} \left[\frac{X_{\kappa}}{\kappa} \right] = \gamma_1 \rho_{\kappa}, \quad \underline{X_{\kappa}} := \underline{x_1} + \dots + \underline{x_{\kappa}}$$

$$\gamma_{(\kappa)} = \frac{\gamma_{(1)}}{\kappa^{2-2H}}$$

γ = variance (var)

κ = time scale

H = Hurst parameter

γ_(κ) = climacogram

ρ_(κ) = dimensionless climacogram

The selection of climacogram for the estimation of the Hurst parameter was applied since it functions as the most statistical reliable tool towards the stochastic explanation of geophysical processes, compared to the widely-used auto-covariance and power spectrum^[9].

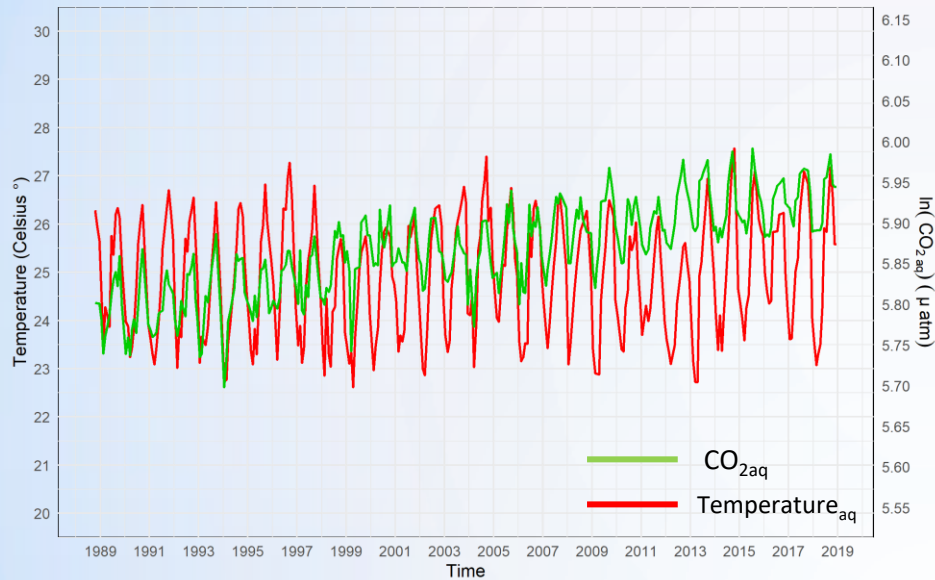
Classification of temporal phenomenona based on Hurst^[8]

- $H > \frac{1}{2}$: ***persistence***
- $H = \frac{1}{2}$: ***white noise (purely random process)***
- $H < \frac{1}{2}$: ***anti – persistence***

Time-series Analysis (1)

CO_{2aq} ~ Temperature

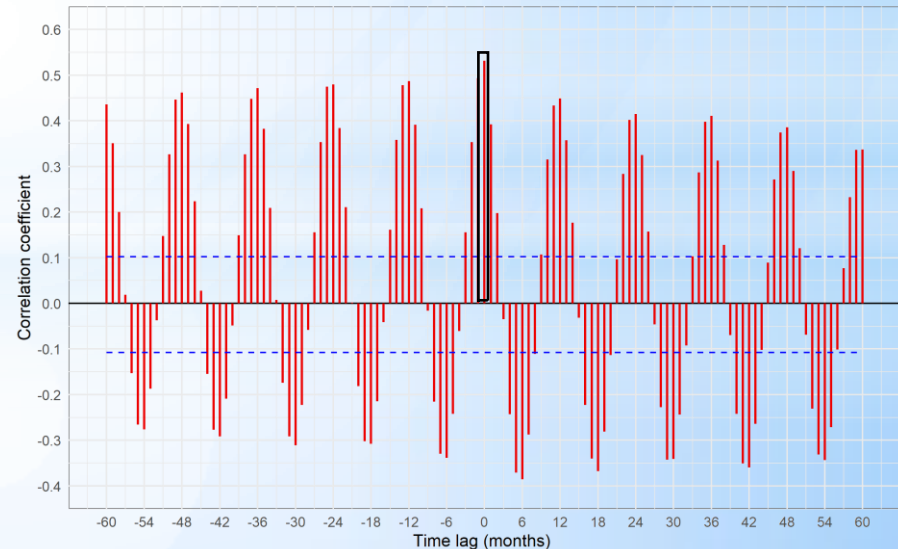
Time series of aquatic CO_{2aq} (μatm) and Temperature (HOT) measurements (1988-2018)



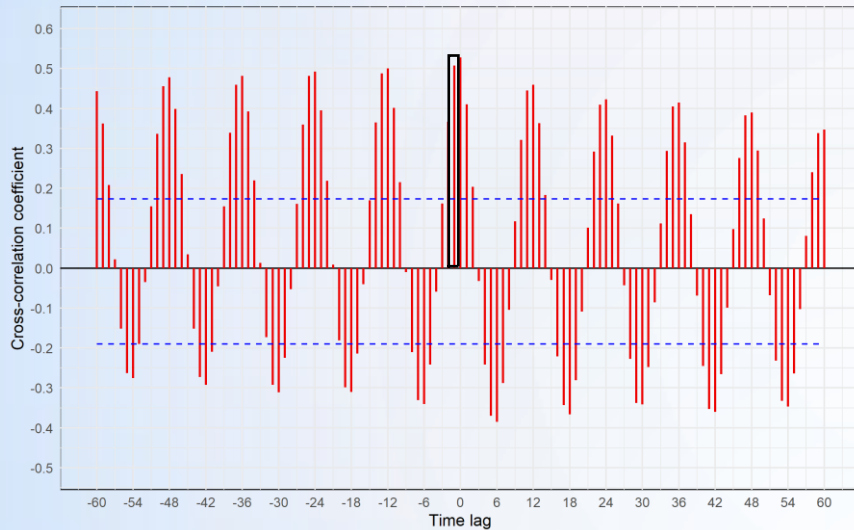
In the original time series of the ocean **carbon dioxide** (natural logarithm transformation^[7]) and **temperature** measurements it is apparent that during the last 30 years there is a discrete increasing trend of **CO_{2aq}**, while temperature exhibits a more erratic behavior. Both processes appear to be under a strong seasonal effect, a behavior that will be further analyzed in the following sections.

In the CCF plot between the original observations of aquatic **CO_{2aq}** (x) and **temperature** (y) the highest positive value has been attained at lag zero (+0.53) and it keeps a decreasing periodic positive and negative peak in a sequence of 6 and 12 lag (months), respectively. There is a significant cross-symmetric behavior around lag zero and the periodic peaks indicate a seasonal phenomenon^[5]. Additionally, causality cannot be explained through the above graphs^[7].

Cross-correlation of CO_{2aq} (μatm) and Temperature measurements (Hawaii Ocean Time Series 1988-2018)

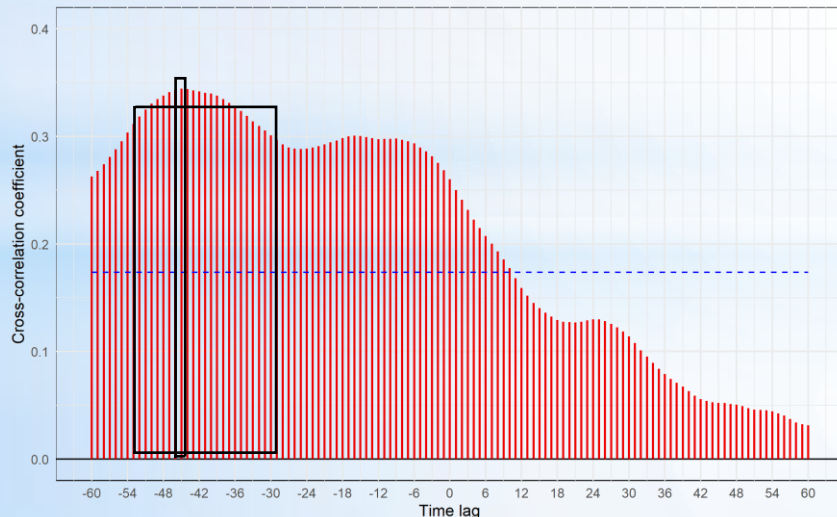


Cross-correlation of 2 month Moving Average of CO_{2aq} (μ atm) and Temperature measurements
(Hawaii Ocean Time Series 1988-2018)



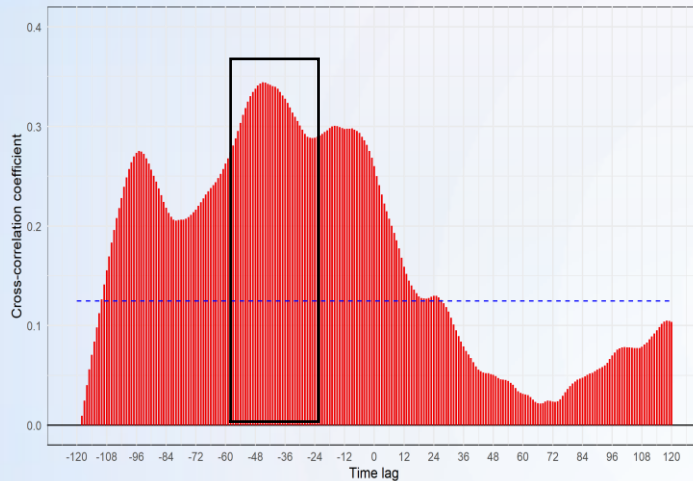
With the application of a 2-month moving average (2 month lag) on the aquatic CO_{2aq}(x) and temperature (y), the seasonal periodicity is still apparent with the highest positive value recorded at lag zero (+0.52).

Cross-correlation of 12 month Moving Average of CO_{2aq} (μ atm) and Temperature measurements
(Hawaii Ocean Time Series 1988-2018)



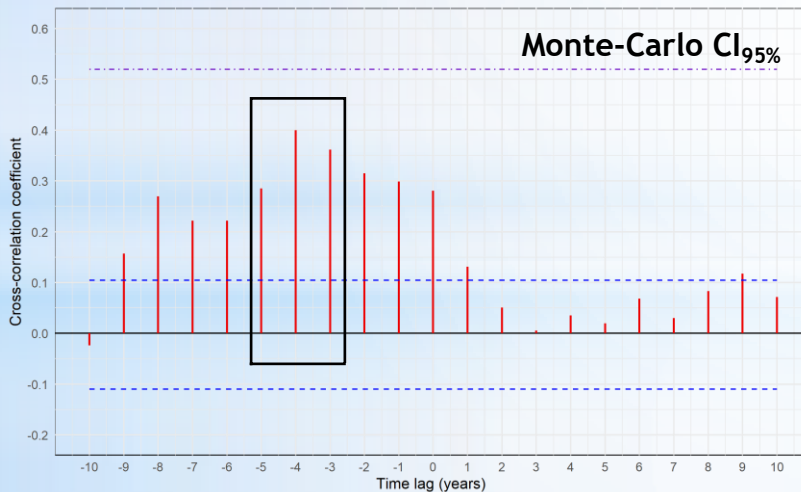
The annual (12-month) moving average showed an interesting behavior, with an increasing and exclusively significant CCF at negative lags, with the maximum observed at the lag -45 (~4 years) with a positive value of +0.34.

Cross-correlation of 12 month Moving Average of CO_{2aq} (μatm) and Temperature measurements
(Hawaii Ocean Time Series 1988-2018)



In order to verify whether if the CCF values occur at larger lags, we investigated the behavior in a larger lag-window (+120,-120) and **we concluded that, indeed, the time lag range (months) from -37 to 47 (3y-4y) had the highest CCF observations in both processes.**

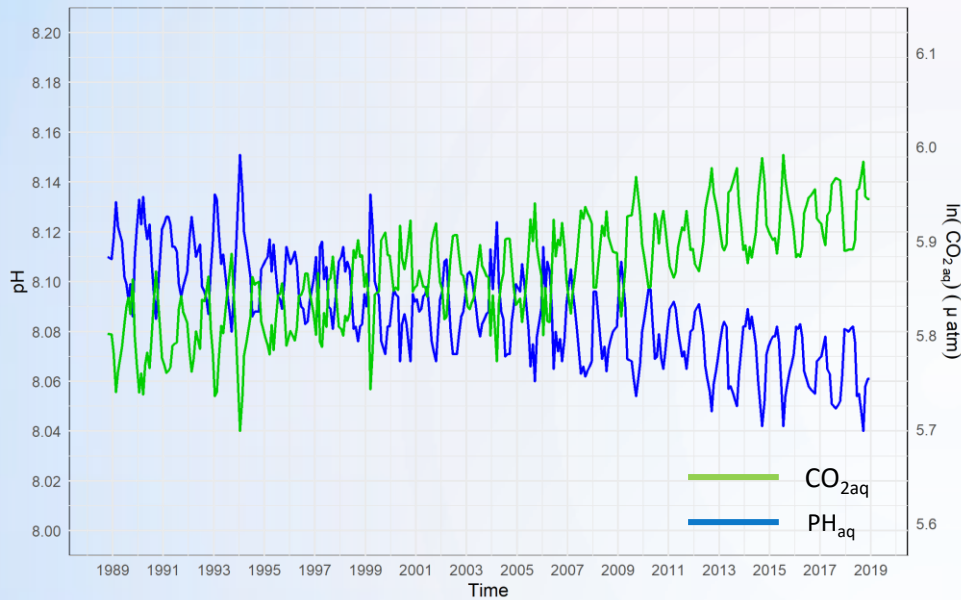
Cross-correlation of Annual Average of CO_{2aq} (ppmv) and Temperature
(Hawaii Ocean Time series 1988-2018)



Apparently, with the application of a MSC in a AR(1) model based on the statistical characteristics of annual **CO_{2aq}** and **temperature**, the observed directionality **was not statistical significant** at 95% of confidence intervals.

Time-series Analysis (1)

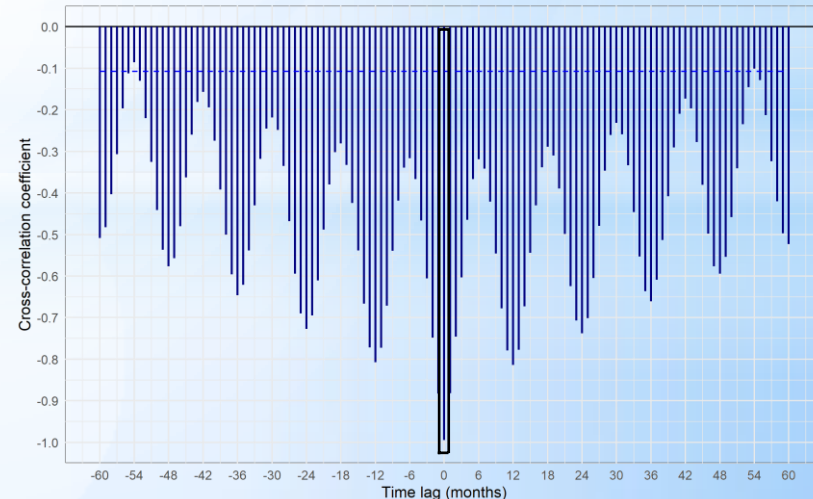
Time series of aquatic $\text{CO}_{2\text{aq}}$ (μatm) and PH (HOT) measurements (1988-2018)



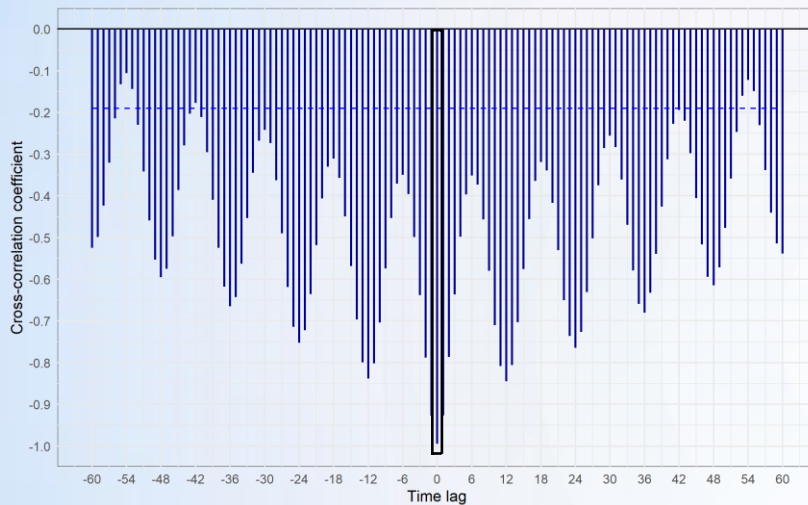
In the original time series of the ocean **carbon dioxide** (natural logarithm transformation ^[7]) and **pH** measurements there is a clear reflecting mirroring effect between the interaction of both variables.

In the CCF between the original observations of aquatic **pH** (x) and **carbon dioxide** (y) the highest negative value has been attained at lag zero (-0.99) and it keeps a decreasing negative periodic peak in a standard sequence of 12 lag (months). There is a significant symmetric behavior around lag zero and the periodic peaks indicate a synchronous seasonal interaction of processes.

Cross-correlation of PH and $\text{CO}_{2\text{aq}}$ (μatm) measurements
(Hawaii Ocean Time Series 1988-2018)

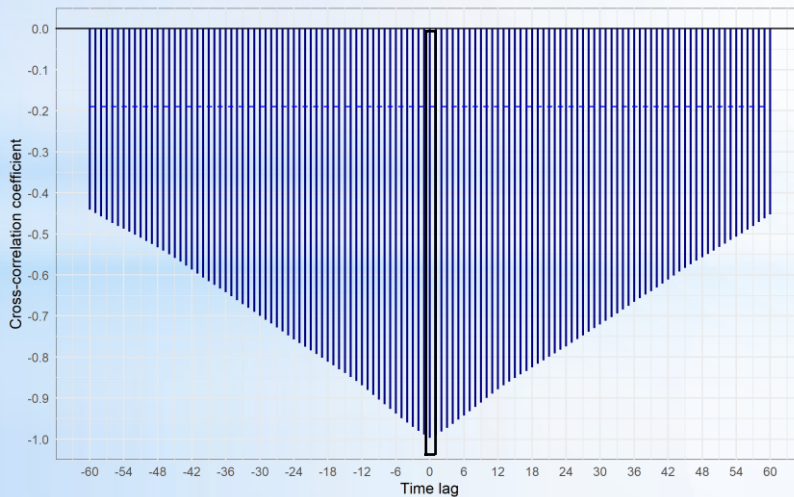


Cross-correlation of 2 month Moving Average of PH and $\text{CO}_{2\text{aq}}(\mu\text{atm})$ measurements
(Hawaii Ocean Time Series 1988-2018)



At a next phase, the 2-month moving average on the aquatic **pH** (x) and **carbon dioxide** (y) resulted in significant negative correlations with the maximum CCF value recorded at lag zero (-0.99). Additionally, there is a seasonal periodic cycle with subsequent decreasing negative peaks towards larger positive and negative lags.

Cross-correlation of 12 month Moving Average of PH and $\text{CO}_{2\text{aq}}(\mu\text{atm})$ measurements
(Hawaii Ocean Time Series 1988-2018)

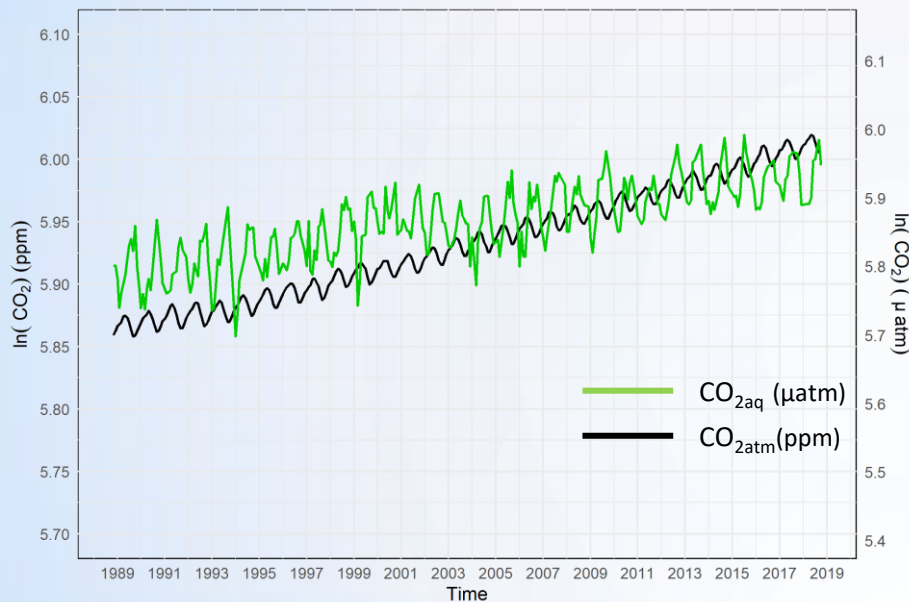


The annual (12-month) moving average sustained the symmetric negative correlation at lag zero (-0.99), a consistent behavior with the previous analyses.

Time-series Analysis (1)

$$\text{CO}_{2\text{aq}} \sim \text{CO}_{2\text{atm}}$$

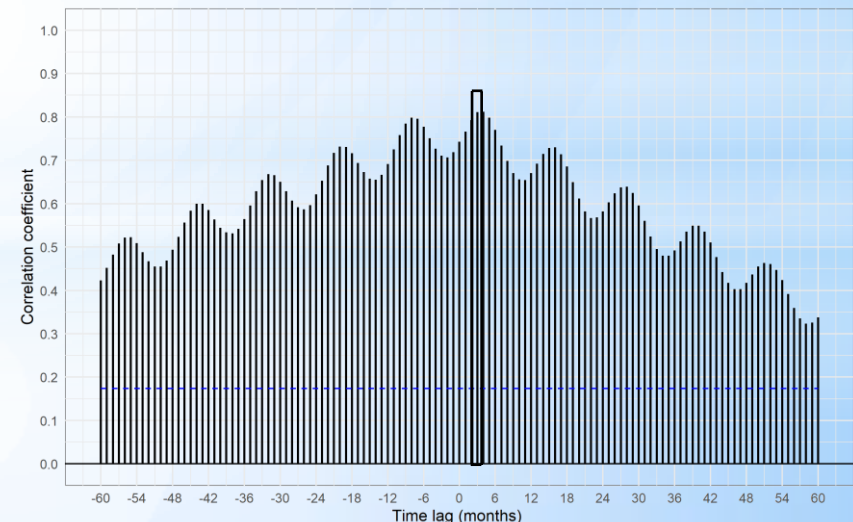
Time series of atmospheric $\text{CO}_{2\text{atm}}(\text{ppm})$ (NOAA) and aquatic $\text{CO}_{2\text{aq}}(\mu\text{atm})$ (HOT) measurements (1988-2018)



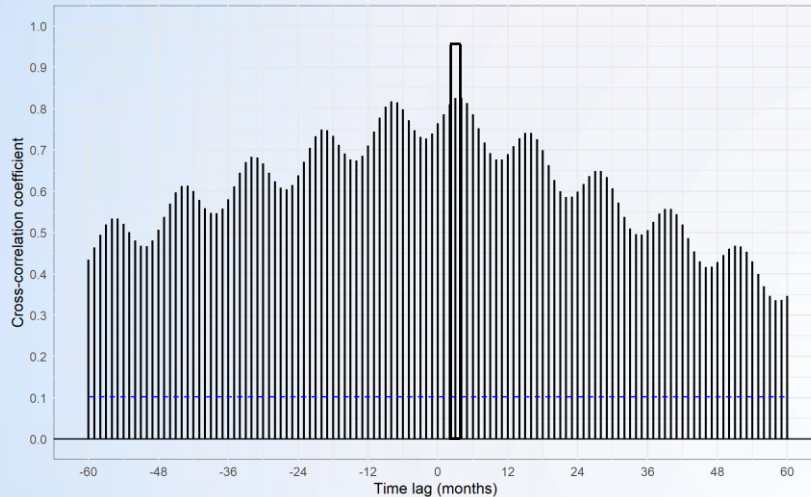
Based on the of the **aquatic** and **atmospheric** carbon dioxide (natural logarithm transformation^[7]) measurements, a common increasing process occurs. Atmospheric observations demonstrated a steady positive escalation while aquatic carbon dioxide time series exhibited a similar, though variant, behavior.

The highest positive value in the CCF analysis between the original observations of **aquatic** (x) and **atmospheric** (y) carbon dioxide, was recorded at the 4th lag (+0.81) and therefore, there is a positive periodic peak in a sequence of an annual lag (12 months). Regarding larger time lags, the interaction is characterized as significant symmetric behavior around the fourth lag and once more, the periodic peaks indicate the presence of a seasonal phenomenon^[5].

Cross-correlation of $\text{CO}_{2\text{aq}}(\mu\text{atm})$ HOT and $\text{CO}_{2\text{atm}}(\text{ppm})$ Mauna Loa measurements

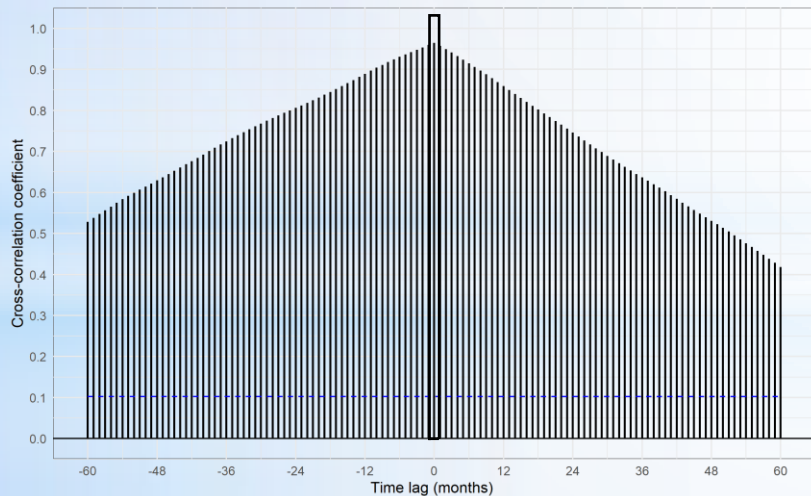


Cross-correlation of 2 month Moving Average of $\text{CO}_{2\text{aq}}(\mu\text{atm})$ HOT and $\text{CO}_{2\text{atm}}(\text{ppm})$
Mauna Loa measurements



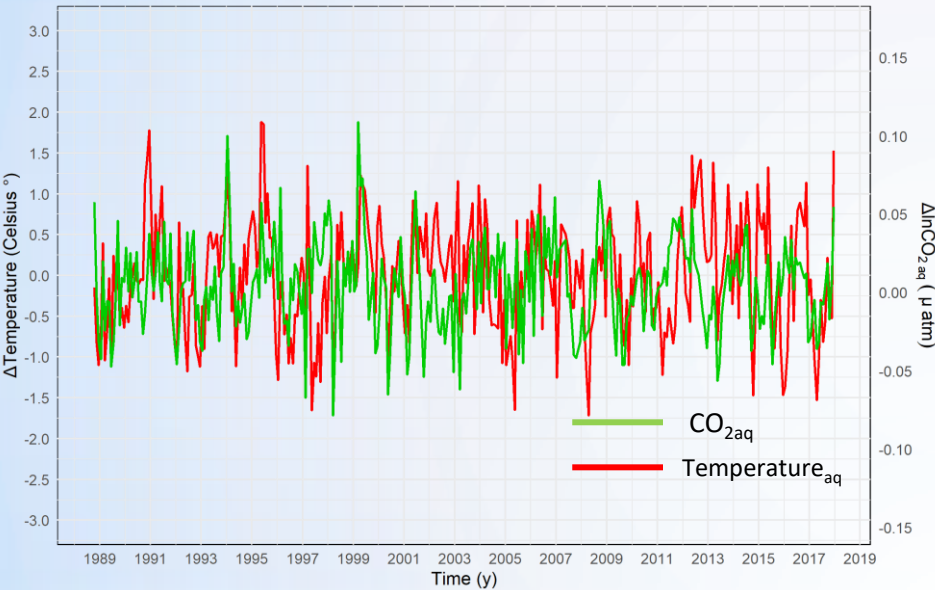
Similarly, the 2-month moving average (2 month lag) on the **aquatic** (x) and **atmospheric** (y) carbon dioxide exhibited significant seasonal periodicity around the 4th lag, with the CCF calculated the maximum CCF value (+0.81).

Cross-correlation of 12 month Moving Average of $\text{CO}_{2\text{aq}}(\mu\text{atm})$ HOT and $\text{CO}_{2\text{atm}}(\text{ppm})$
Mauna Loa measurements

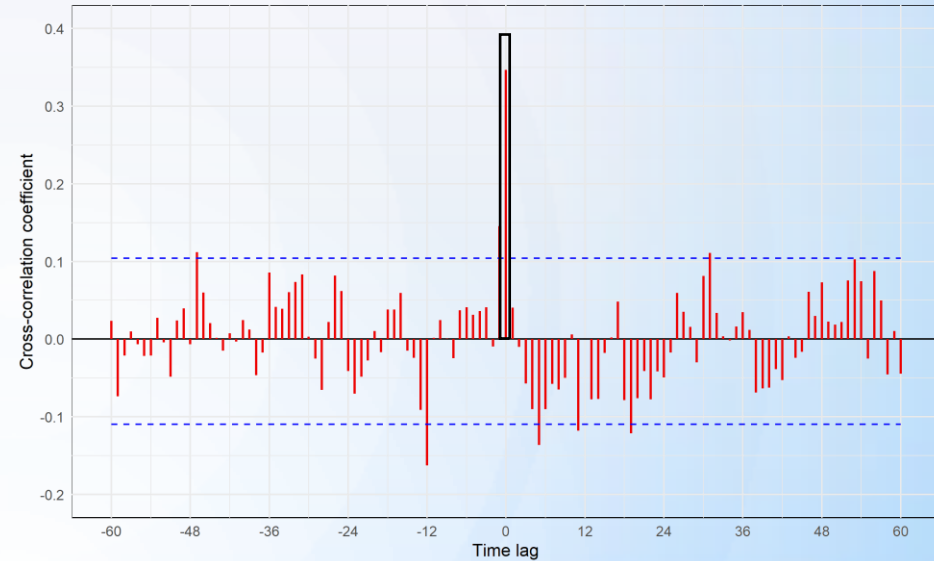


The annual (12-month) moving average between both processes showed a typical symmetric positively correlated interaction at zero lag (+0.96). Hence, the annual correlation is slightly greater than the effect of the monthly observations.

Time series of aquatic $\Delta\text{CO}_{2\text{aq}}$ (μatm) and Δ Temperature (HOT) measurements (1988-2018)

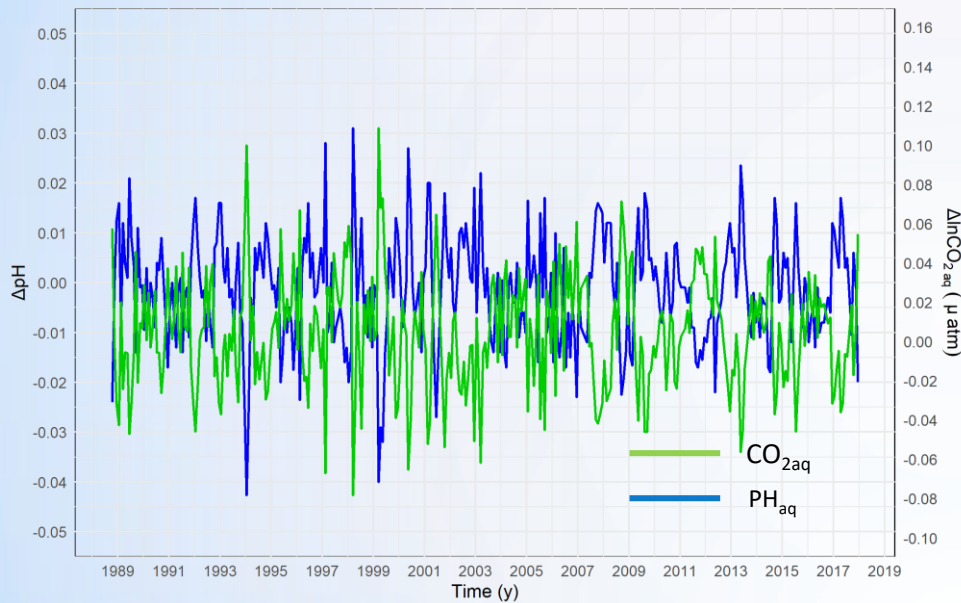


Cross-correlation of monthly $\Delta\text{CO}_{2\text{aq}}$ (μatm) and Δ Temperature measurements (Hawaii Ocean Time Series 1988-2018)

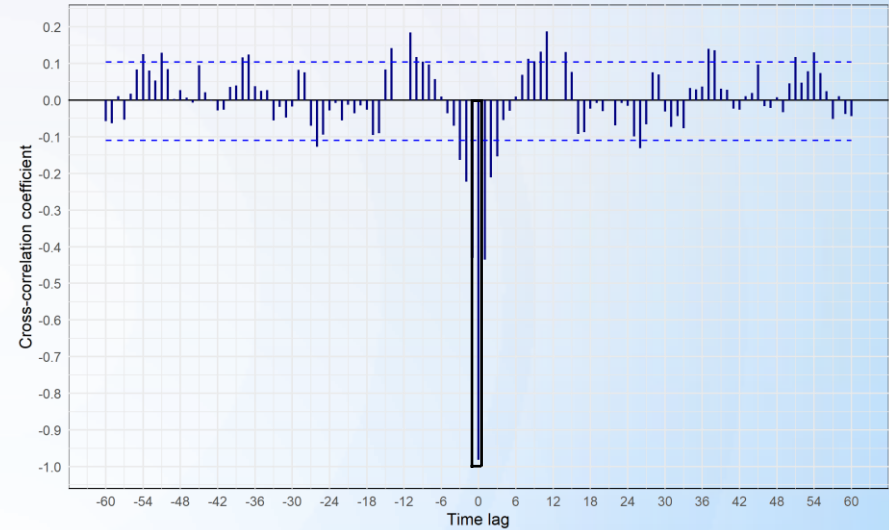


With the elimination of the periodicity effect on the processes, the annual difference (f.e. 1st PH value: $\text{PH}_{\text{Oct}_{1989}} - \text{PH}_{\text{Oct}_{1988}}$), ocean **carbon dioxide** and **temperature** measurements showed that there is not a clear pattern in the succession of events. This can be validated with the CCF plot, indicating that the highest value recorded at lag zero (+0.34) with a **non significant pattern** alongside the zero point, thus highlighting the erratic behavior of temperature in the original time series.

Time series of aquatic $\Delta \text{CO}_{2\text{aq}}$ (μatm) and ΔPH (HOT) measurements (1988-2018)



Cross-correlation of monthly $\Delta \text{CO}_{2\text{aq}}$ (μatm) and ΔPH measurements (Hawaii Ocean Time Series 1988-2018)



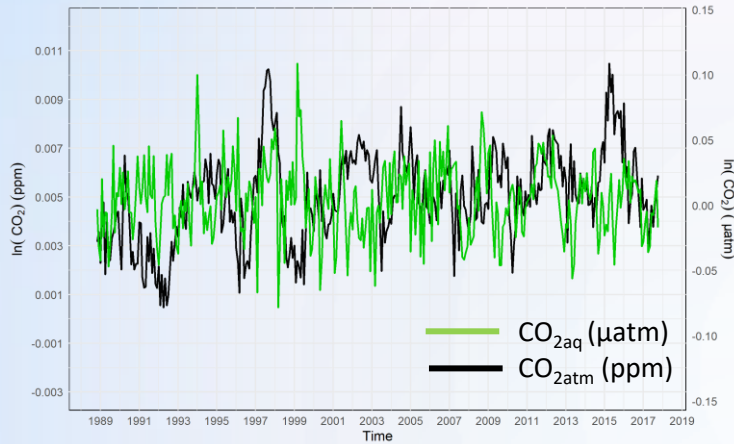
Contrarily, the Δ -transformed time-series of aquatic **pH** and **carbon dioxide** difference, resulted in the same reflected mirrored behavior of the time series. Furthermore, the cross-correlation of both variables strongly support the original time-series behavior with a clear **symmetric** pattern. The maximum value (lag zero) of the CCF was recorded at -0.98.

Time-series Analysis (2)

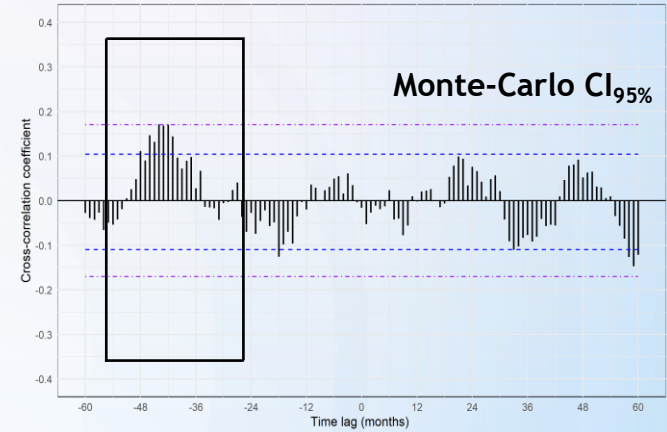
$$\Delta\text{CO}_{2\text{atm}} \sim \Delta\text{Temperature}$$

$$\Delta\text{CO}_{2\text{aq}} \sim \Delta\text{CO}_{2\text{atm}}$$

Time series of atmospheric $\Delta\text{CO}_{2\text{atm}}$ (ppm) (NOAA) and aquatic $\Delta\text{CO}_{2\text{atm}}$ (μatm) (HOT) measurements (1988-2018)

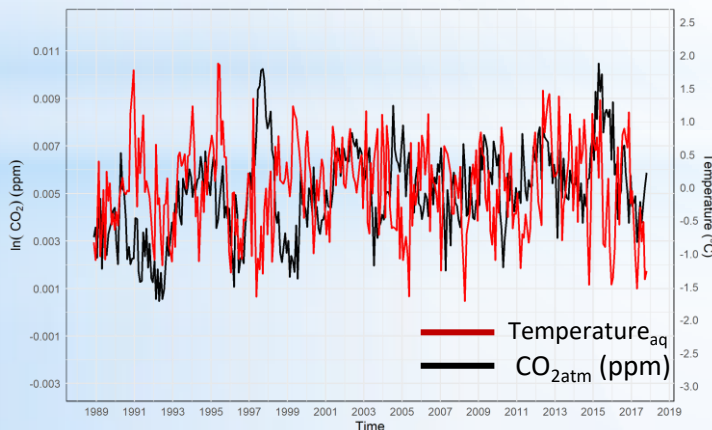


Cross-correlation of Annual $\Delta\text{CO}_{2\text{aq}}$ (ppmv) HOT and $\Delta\text{CO}_{2\text{atm}}$ (ppmv) Mauna Loa measurements

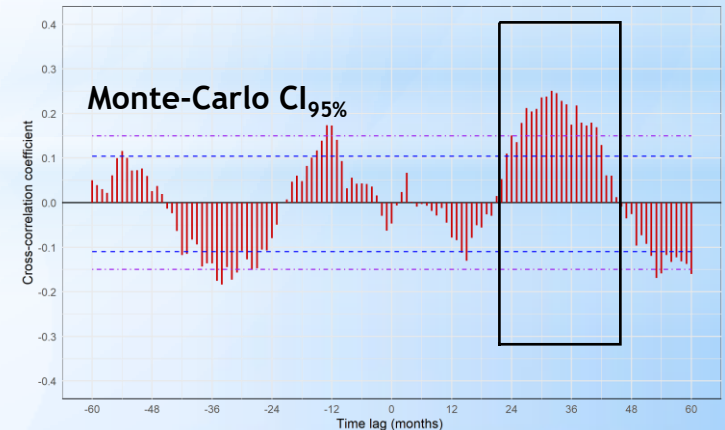


The differences between the $\text{CO}_{2\text{aq}}$ and $\text{CO}_{2\text{atm}}$, demonstrated a clear pattern of a negligible statistical significance between the two processes, except an allocated time-lag grouping at -40 to -45 time lag (months) which was partially-rejected through the MSC $\text{CI}_{95\%}$ thresholds. Since temperature showed an interesting behavior in the previous section we tested its difference (Δ) related with the $\Delta\text{CO}_{2\text{atm}}$ and it appeared that there's a **validated and statistical significant directionality of $T \rightarrow \text{CO}_{2\text{atm}}$** with a ~ 2.5 year lag.

Time series of atmospheric $\Delta\text{CO}_{2\text{atm}}$ (ppm) (NOAA) and aquatic $\Delta\text{Temperature}$ (HOT) measurements (1988-2018)



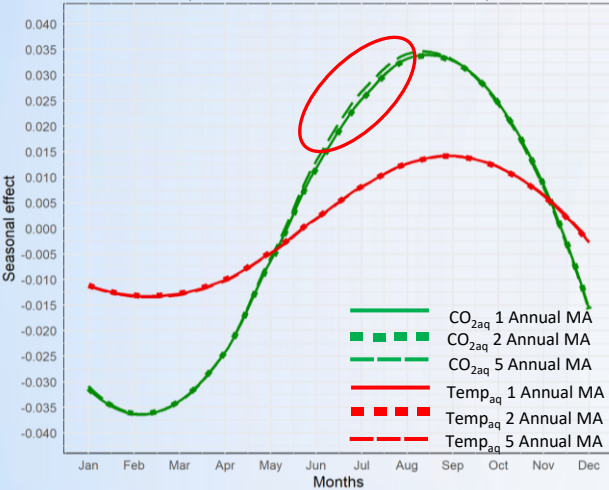
Cross-correlation of Annual $\Delta\text{CO}_{2\text{atm}}$ (ppmv) (NOAA) and $\Delta\text{Temperature}$ (°C) Mauna Loa measurements



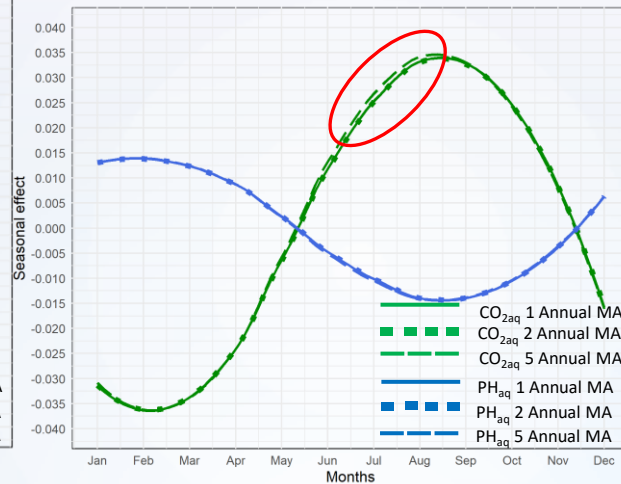
Time-series Analysis (3)

Seasonality effect

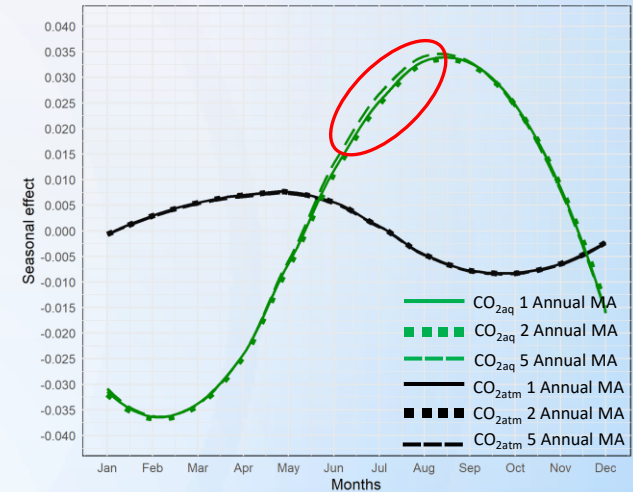
Seasonal effect on $\text{CO}_{2\text{aq}} (\mu\text{atm} \cdot 10^{-2})$ and Temperature ($^{\circ}\text{C}$) measurements
(Hawaii Ocean Time Series 1988-2018)



Seasonal effect on PH and $\text{CO}_{2\text{aq}} (\mu\text{atm})$ measurements
(Hawaii Ocean Time Series 1988-2018)

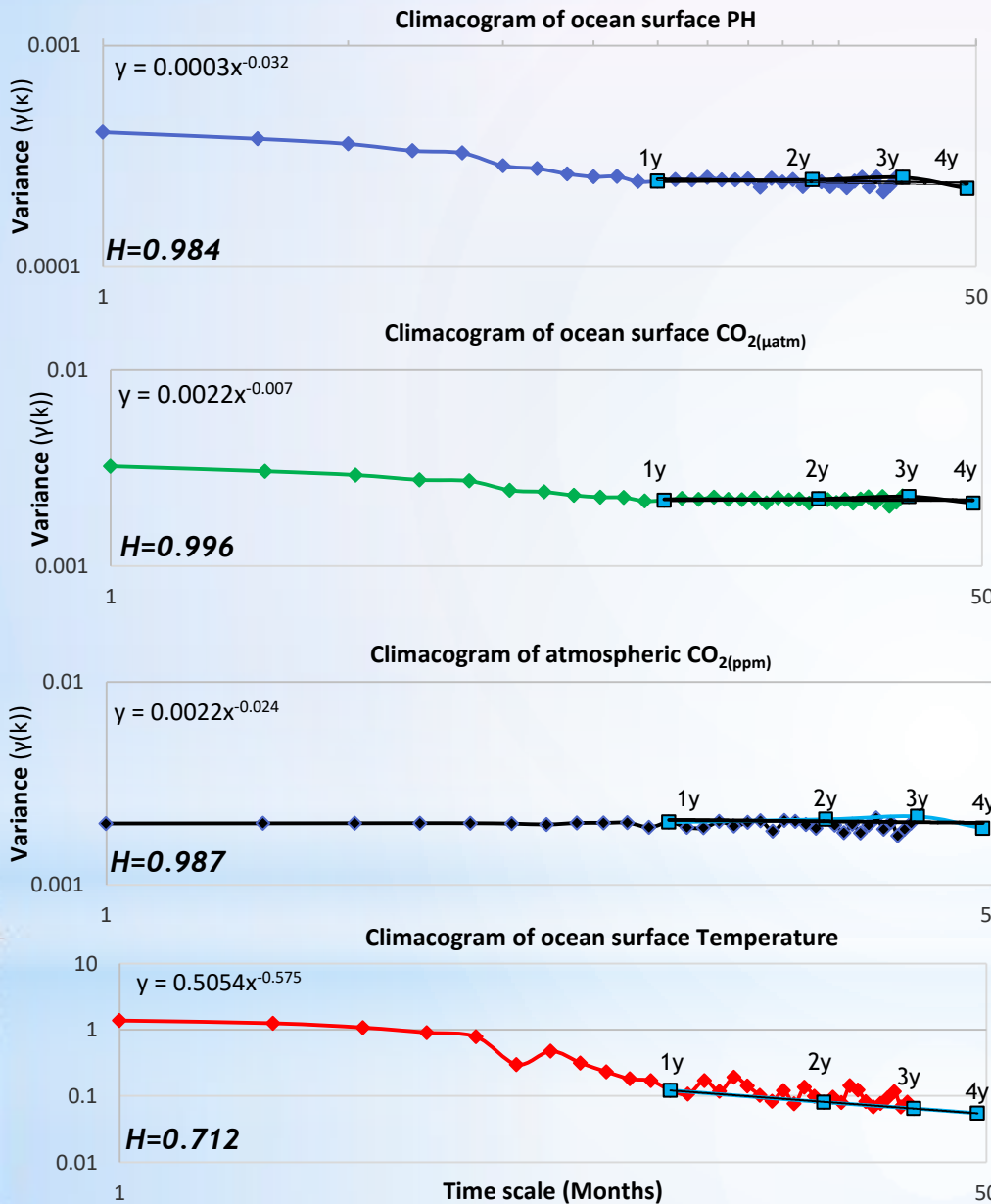


Seasonal effect on $\text{CO}_{2\text{aq}} (\text{ppm})$ and $\text{CO}_{2\text{aq}} (\mu\text{atm})$ measurements
(Hawaii Ocean Time Series 1988-2018)



Since seasonality was highlighted as a crucial component in the behavior of the phenomenon, we extracted gradual increasing annual (1;2;5 years) moving averages (MA) from the original time-series, and we estimated the monthly average effect on the observations units. In the case of aquatic **temperature** and $\text{CO}_{2\text{aq}}$, both variables had a common phase with the highest positive peak between August-September and lowest in February. Correspondingly, **pH** had the exact opposite phase compared to the $\text{CO}_{2\text{aq}}$ with the highest peak in February and lowest in September. The, exclusively seasonal effect, 4-month phase lag of the **air-ocean** CO_2 transferability was confirmed since the highest peak of $\text{CO}_{2\text{atm}}$ appeared to be in May and the lowest between September-October.

It is worth mentioning that the different applied moving average (MA) extractions appeared to show equal behavior, with the 5th MA having a slight divergence during summer months (June-August).



Finally, we implemented the empirical climacogram for all the variables during the examination of processes on the phenomenon of OA (log transformed γ_k axis). Hurst parameter was estimated according to the power type slope of the annual scale (1-4 years) so as to exclude the non-desired effects of periodicity in monthly scale. **Overall, the 4 parameters showed $H > 1/2$ which demonstrates temporal persistence**^[7,10].

More specifically, the annual H parameter for aquatic **pH**, **$CO_{2(aq)}$** , **$CO_{2(atm)}$** obtained from the 30 year range time-series exhibited large values approximate to 1 ($H > 0.98$). However, aquatic **temperature** presented a less similar behavior on annual scales as an irregular stochastic process.

Main findings –Conclusions

- Analyses of time-series related to OA concluded that the increase of $p\text{CO}_{2\text{aq}}$ was similar to the $p\text{CO}_{2\text{atm}}$ ^[11]. In the present analysis we discovered an interannual 4 month phase difference between both variables which was eliminated after the extraction of seasonality through appropriate procedures. The annual differences thereof exhibited a ~ 4 year lag with directionality $\text{CO}_{2\text{atm}} \rightarrow \text{CO}_{2\text{aq}}$ which however is statistically non-significant (tested by MCS).
- An interesting observation was the detection of a statistically significant, assessed through stochastic simulation, **~ 2.5 year lag** in the annual differences (Δ), in the processes of $T_{\text{aq}} \rightarrow \text{CO}_{2\text{atm}}$. The directionality is consistent with the results of a previous study on atmospheric $T_{\text{atm}} \rightarrow \text{CO}_{2\text{atm}}$ with a ~ 1 year lag **in an annual scale**^[7].
- The relationship between **pH** and $\text{CO}_{2\text{aq}}$ resulted in a reflecting-mirrored interaction, which is confirmed by previous studies^[1,12]. Regarding the observed seasonality, **pH** seasonal variation appeared to be in agreement with previous analysis in the region^[1].
- **Strong persistence ($H \gg 1/2$) was detected in all the examined variables**, which indicates strong clustering (grouping) of similar values, enhanced change and uncertainty, a quite common behavior in natural processes^[7,10].
- A negative effect of OA is the **possibility that it can impact aquatic populations of shell-forming organisms**^[1,14]. These ocean chemical alternations may cause progressive negative feedback response, starting from the population level to marine ecosystems as a whole.
- The present study was focused on a single site dataset. However, there exist site-specific differences on a global scale^[11,12], along with a variability of biological responses and vulnerability to OA related with the latitude location of each case-study^[1,13]. Except the geospatial variance, the interaction of impacts has been found to be diverging during the life-history (development) stages of an organism^[14].
- Based on the findings of this work, it appears that there may exist an **interesting interdisciplinary research arena in the interaction between trends and seasonality effects on the response of marine biota**. This evolutionary concept of adaptivity, described as the “phenotypic plasticity”^[15], may function towards the mitigation of the severe effects of environmental stressors related to OA.

References

- [1]: Doney, S. C., Fabry, V. J., Feely, R. A., & Kleypas, J. A. (2009). Ocean Acidification: The Other CO₂ Problem. *Annual Review of Marine Science*, 1(1), 169–192. <https://doi.org/10.1146/annurev.marine.010908.163834>
- [2]: Dore, J.E., R. Lukas, D.W. Sadler, M.J. Church, and D.M. Karl. (2009). Physical and biogeochemical modulation of ocean acidification in the central North Pacific. *Proceedings of the National Academy of Sciences USA* 106:12235-12240.
- [Download data \(.txt\)](#)
- [3]: Thoning, K.W., Crotwell, A.M. and Mund, J.W. (2021). Atmospheric Carbon Dioxide Dry Air Mole Fractions from continuous measurements at Mauna Loa, Hawaii, Barrow, Alaska, American Samoa and South Pole. 1973-2019, Version 2021-02 National Oceanic and Atmospheric Administration (NOAA), Global Monitoring Laboratory (GML), Boulder, Colorado, USA <https://doi.org/10.15138/yaf1-bk21>
- [Download data \(.txt\)](#)
- [4]: Bayen, A. M., Siauw, T. (2015). An Introduction to MATLAB® Programming and Numerical Methods for Engineers. 2015, p. 211-223 . Chapter 14 – Interpolation.
- [5]: Venables, W. N. and Ripley, B. D. (2002). *Modern Applied Statistics with S*. Fourth Edition. Springer-Verlag. Time Series Analysis. p. 390
- [6]: Holmes, E. E., M. D. Scheuerell, and E. J. Ward, (2021). Applied time series analysis for fisheries and environmental data. NOAA Fisheries, Northwest Fisheries Science Center, 2725 Montlake Blvd E., Seattle, WA 98112.
- [7]: Koutsoyiannis, D., & Kundzewicz, Z. W. (2020). Atmospheric Temperature and CO₂: Hen-Or-Egg Causality? *Sci*, 2(4), 83. <https://doi.org/10.3390/sci2040083>
- [8]: Koutsoyiannis, D. (2020). Stochastics of Hydroclimatic, Extremes A Cool Look at Risk. <https://www.itia.ntua.gr/en/docinfo/2000/>
- [9]: Dimitriadis, P., & Koutsoyiannis, D. (2015). Climacogram versus autocovariance and power spectrum in stochastic modelling for Markovian and Hurst–Kolmogorov processes. *Stochastic Environmental Research and Risk Assessment*, 29(6), 1649–1669. <https://doi.org/10.1007/s00477-015-1023-7>
- [10]: Dimitriadis, P., Koutsoyiannis, D., Iliopoulou, T., & Papanicolaou, P. (2021). A Global-Scale Investigation of Stochastic Similarities in Marginal Distribution and Dependence Structure of Key Hydrological-Cycle Processes. *Hydrology*, 8(2), 59. <https://doi.org/10.3390/hydrology8020059>
- [11]: Takahashi, T., Sutherland, S. C., Feely, R. A., & Wanninkhof, R. (2006). Decadal change of the surface water pCO₂ in the North Pacific: A synthesis of 35 years of observations. *Journal of Geophysical Research*, 111(C7). <https://doi.org/10.1029/2005jc003074>
- [12]: Bates, N., Astor, Y., Church, M., Currie, K., Dore, J., Gonaález-Dávila, M., Lorenzoni, L., Muller-Karger, F., Olafsson, J., & Santa-Casiano, M. (2014). A Time-Series View of Changing Ocean Chemistry Due to Ocean Uptake of Anthropogenic CO₂ and Ocean Acidification. *Oceanography*, 27(1), 126–141. <https://doi.org/10.5670/oceanog.2014.16>
- [13]: Hofmann, G. E., Barry, J. P., Edmunds, P. J., Gates, R. D., Hutchins, D. A., Klinger, T., & Sewell, M. A. (2010). The Effect of Ocean Acidification on Calcifying Organisms in Marine Ecosystems: An Organism-to-Ecosystem Perspective. *Annual Review of Ecology, Evolution, and Systematics*, 41(1), 127–147. <https://doi.org/10.1146/annurev.ecolsys.110308.120227>
- [14]: Byrne, M., & Fitzer, S. (2019). The impact of environmental acidification on the microstructure and mechanical integrity of marine invertebrate skeletons. *Conservation Physiology*, 7(1). <https://doi.org/10.1093/conphys/coz062>
- [15]: Munday, P. L., Warner, R. R., Monro, K., Pandolfi, J. M., & Marshall, D. J. (2013). Predicting evolutionary responses to climate change in the sea. *Ecology Letters*, 16(12), 1488–1500. <https://doi.org/10.1111/ele.12185>